Validated AE Application for Continuous Monitoring of the Structural Condition of the Supporting Structure of Offshore Wind Turbines

Ángela ANGULO[1], Jamil KANFOUD[1], Yoann LAGE[1], Catherine HERVÉ[2], Slim SOUA[1], Guillaume PERRIN[2], Tat-Hean GAN[1]

[1]TWI Ltd, Condition and Structural Health Monitoring, Integrity Management Group. Granta Park, Great Abington, CB21 6AL – Cambridge (UNITED KINGDOM) angela.angulo@twi.co.uk, slim.soua@twi.co.uk, jamil.kanfoud@twi.co.uk, yoann.lage@twi.co.uk, tat-hean.gan@twi.co.uk
[2]CETIM, 52 Avenue Félix Louat, CS 80067, Senlis Cedex, 60304 (FRANCE)
catherine.herve@cetim.fr, guillaume.perrin@cetim.fr

Abstract

It is widely accepted that the use of acoustic emission technology offers unique advantages for the inspection and structural health monitoring of structures. Even though this method is quite evolved, there are still challenges in its application largely due to its complex behaviour and there are also other factors to consider such as numerous possible vibrational modes, dispersion, attenuation, noise and multiple reflections etc. There are also challenges in the use of this technology for offshore structures especially when the structures are totally submerged in water and when there are different materials used for construction. In order to address these issues and determine the applicability of these methods, a study has been carried out that uses finite element analysis and an experimental study to understand their behaviour in an offshore wind turbine monopole has also been conducted.

Keywords: Structural Health Monitoring, Offshore Wind Turbine, Acoustic Emission, Structural Integrity, Wind Energy, Renewables

1. INTRODUCTION

Offshore structures, such as wind turbine monopiles are subjected to cyclic loads and harsh marine environments resulting in fatigue damage, cracks and corrosion. These defects can remain unnoticed and undetected until there is a catastrophic failure. It is therefore highly desirable to monitor the structural integrity of these assets throughout the entire life cycle. This paper addresses the issues and capabilities of ultrasonic inspection for the health monitoring of offshore wind turbine monopile structures.

Acoustic Emission (AE) is as a non-destructive inspection method which has already been used in the offshore industry [1]. The objective of this study is to investigate the ability of AE to detect defects such as debonding of the grout and steel and the capability of the sensors in detecting cracks and crack propagation within the turbine structure. Numerical simulation and experiments were conducted to identify the wave propagation and attenuation through the grout.

1.2 Degradation mechanism and monitoring techniques

Monopile foundation structures have been used for offshore oil and gas platform foundations for decades. They are also known as pile-sleeve connections. A pile-sleeve connection consists of a sleeve mounted concentrically on a pile that is driven into the seabed, with the larger diameter sleeve placed around the smaller diameter pile forming annuli between them.

The connection is fixed by filling these annuli with a specially developed grout that settles into a high strength concrete (Figure 1). This technology has been transferred to offshore wind turbines by utilizing the improved properties of the reinforced grout. The sleeve related to wind turbines is also known as a transition piece as it joins the wind turbine tower to the pile.

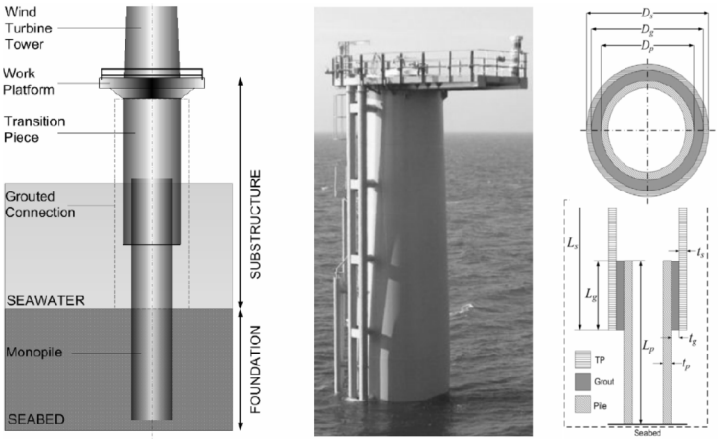

Figure 1: Grouted connection illustration and representation of the grouted connection.

The monopile foundation is divided into two regions; the substructure is the structure between the wind turbine tower and seabed, while the actual foundation is the structure that penetrates the seabed.

1.2.1 Damage mechanisms

In the early days of offshore wind, the grouting technique was adopted as a supposed quicker and cheaper method of allowing turbine towers to be placed close to vertical on non-vertically installed driven monopiles. Prior to this, bolted flanged connections had been used at the initial offshore sites.

Failures are primarily due to the widespread non-use of shear keys, a series of horizontal rings of welded steel beads, spaced tens of centimetres apart, placed on the inner surface of the tubular steel transition piece and the outer monopile surface. Since severe lateral cyclic bending occurs during extreme wind and wave loading conditions, the dead weight is proportionally much lower and bending predominates. As a result, this leads to periodic tensile stressing of the compressively strong but extremely brittle grouts, which eventually crack and crumble. This can result in failure, settlement, tower tilting and the structure frequently ending up resting on internal support brackets which are not designed for that purpose.

The stress cycles that result in fatigue on wind turbine towers is very complex, due to the combination of effects from wind, waves and currents and the vibration of the turbine in the nacelle. Cracks may develop where there is a concentration of stresses, usually where there is an abrupt change in geometry, such as a notch. Where grouting has failed and the transition piece has slipped onto the brackets that were used to support the tower during erection, fatigue cracks have been found on the fillet weld that attach the supports to the inside surface of the tower, The fillet weld to the flange is also a possible site for fatigue crack initiation.

1.2.2 Monitoring techniques

Acoustic Emission (AE) is considered as the primary SHM technique. It is required to detect stress waves from cracks, corrosion and tower slippage in the presence of high levels of

acoustic noise from the tower structure, turbine and the environment (wind and wave action) [2]. Vibration analysis is a secondary SHM technique that uses accelerometers to monitor fatigue crack damage mechanisms such as vibrations caused by the turbine, the environment (wind and wave action) and accidents. The data may also be used to identify noise in the AE.

Guided ultrasonic wave propagation can also be utilised as a supplementary technique to the AE for evaluating the source of AE. By a process of 'time reversal' a sparse array of AE sensors can be activated as GUW transmitters to focus on ultrasound on the AE source using pulse-echo mode. The time-of-flight and amplitude of the echo can be used to locate and measure the size of the source. Modal analysis can also be supplementary to the VA technique, where the accelerometers are able to sense changes in the vibration modes of the whole structure that might indicate gross damage and reduction in overall structural health.

	Acoustic emission	**Vibration analysis**	**Modal analysis**	**Guided ultrasonic waves**
Grout slippage	√	√	√	√
Fatigue cracks	√	√		√
Loose bolts	√	√		√
Corrosion	√			√
Accidental damage	√	√	√	√

Table 1: Summary of structural health monitoring techniques.

2 EXPERIMENTS

The experimental test covers the AE experiments performed on the Ducorit S5 material and the propagation mock-up. The objective of this experiment is to determine the parameters of the acoustic wave's propagation within a 1:1 scale mock-up, representative of a real offshore structure. The acoustic emission instrumentation used for these tests is composed of resonant piezoelectric sensors with a resonance frequency of 200kHz. These sensors convert the mechanical wave's generated through the structure into electrical signals. The coupling to the structure was warranted by silicon grease. The sensors are connected to preamplifiers using connection cables. The preamplifiers have a 34dB gain and ensure filtering and amplification of the electric signals coming from the sensors. This data acquisition system is a multichannel system for characterization and localization of acoustic emission sources with signal filtering within the frequency range 95-850kHz.

2.1 Waves attenuation in Ducorit S5

In order to optimize the positioning of the AE sensors on the mock-up and to give input for the simulations, the attenuation of acoustic waves was measured in a Ducorit S5 sample. An attenuation mock-up was designed and it is represented in
Figure *2*a.

Artificial Hsu-Nielsen sources (pencil lead break) generated at the opposite edge of the mock-up. The acoustic wave generated propagates along the whole length of the structure. Acoustic Emission is measured using AE sensors at regular distances from the source with steps of 10cms. The AE time of arrival determines the acoustic wave velocity and the amplitude allows the determination of the attenuation. The apparition of transversal cracks during the concrete's drying was unfortunately observed. The result of this phenomenon was

that the amplitude recorded on the sensor faces a dramatic drop (≈ -20dBea) pass each crack. For this reason, an extrapolation was made on the attenuation results in order to eliminate the attenuation due to the cracks and only save the one due to material attenuation. The resulting attenuation in the Ducorit S5 was found to be approximately 50dB.m^{-1}, which is consistent with values usually observed in concretes. Results are given in
Figure 2b:

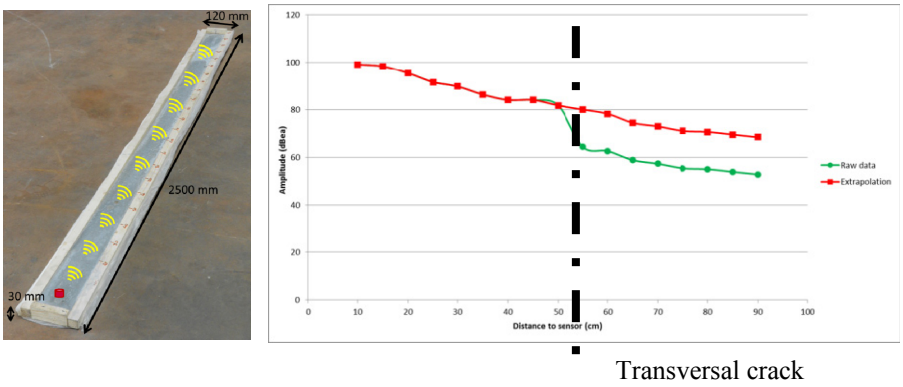

Figure 2a. Design and dimensions – Attenuation mock-up. b. Attenuation results Ducorit S5 – Raw data and extrapolated.

2.2 AE waves propagation

The mock up was built to the design specifications. During drying of the grout, a positioning error of the steel plates led to the debonding of the grout from the monopile (Figure 3). However, experiments were performed in the concrete and at the interface between the grout and the transition piece.

Figure 3: Propagation mock up side and AE sensors coupling.

Firstly, testing was performed on the transition piece to characterize the wave's propagation in the steel plates. Two sensors were positioned on each edge of the plate (spaced by 1240mm) and artificial Hsu-Nielsen sources generated along the plate's length.

As for the Ducorit S5, the attenuation was calculated within the transition piece. Speed was also calculated, taking into account the time correction on the main propagation mode. The calculated speed was thus c ≈ 3150 m.s-1. This speed corresponds to the propagation of a shear wave mode. The attenuation curve for the steel plate in the transition piece attenuation was estimated to be around 11dB.m^{-1}, which is a consistent value for a steel plate. In order to determine precisely the propagation laws within the steel plate, the temporal and frequency analysis of some waveforms was performed. Results showed in Figure 4b are given for an artificial Hsu-Nielsen source generated near the transition piece edge and recorded by both sensors coupled on the structure. The first one is 50mm far from the source, the other one 1290mm far from the source.

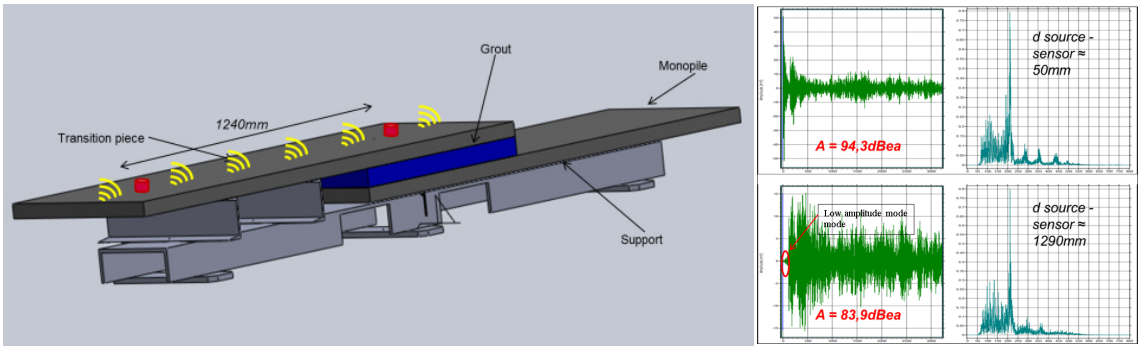

Figure 4a: Propagation tests – Transition piece. 4b: Temporal and frequency analysis – Transition piece.

Two important results concerning the propagation within the steel plate can be observed from these curves:

- For long propagation distances (phenomenon observed from 600mm), a time offset of the burst arrival due to the first low amplitude mode. This phenomenon is responsible of the speed calculation error that must be corrected for valuable measurements;
- No modification of the frequency spectrum of AE bursts through steel.

2.2.1 Propagation in the transition piece

Tests were also performed at the interface between the transition piece and the grout, in order to characterize the wave propagation in the grout and through this interface steel/concrete. Two sensors were positioned on the transition piece, one sensor integrated in the grout during the mock up preparation and as an experimentation one reception sensor coupled to the monopile. A sketch of this test is given in Figure 5:

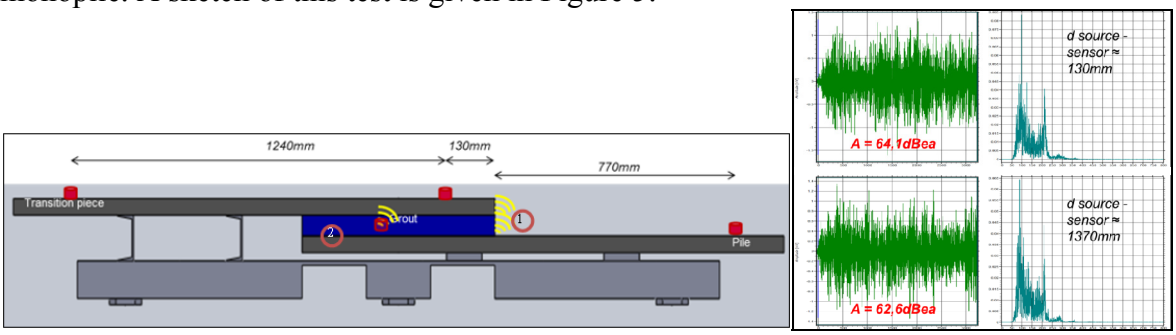

Figure 5: Temporal and frequency analysis – a. Transition piece. b. Transition piece/grout interface.

The wave's propagation speed between the sources generated on the edge of the grout and the sensors placed on the transition speed is about 3700m.s^{-1}. The temporal and frequency analysis of some waveforms have been performed. Results in Figure 5b are given for an artificial Hsu-Nielsen source generated along the grout and recorded by sensors coupled on the transition piece. The first sensor is 130mm from the source, the other one is 1370mm from it. From these curves, two important results regarding the propagation within the steel plate were found. No time offset of the burst arrival due to the first low amplitude mode. It appears that the low amplitude mode has been attenuated enough by the grout to pass below the acquisition threshold. This fact also explains why no time correction is necessary, since the propagation mode first triggering is the main one (highest amplitude). There was also a modification of the frequency spectrum through the grout, with the filtering of high frequencies.

As a final test, the sensor incorporated in the grout was used as an emission sensor in order to determine the variations of the bursts detected on the reception sensors according to the

applied pulse voltage. It was demonstrated that the transmission of acoustic waves from the centre of the grout to the steel plates is possible even for very low tensions (a few volts).

2.3 Conclusion

Based on the results presented in this preliminary report, the following conclusions were found:

- Transmission of acoustic waves through the grout is possible, even in distances higher than 1m. Due to the mock up specifications, it was not possible to evaluate the wave's attenuation on longer distances.
- The waves faced a frequency filtering through the grout and an additional attenuation compared to waves generated on the transition piece.
- The propagation of acoustic waves in the steel plate is very complex since many different modes propagate in the structure. The highest amplitudes are not recorded on the first mode triggering, resulting in a speed calculation error if no time correction is applied.

3. FINITE ELEMENT SIMULATION

The pile and the transition piece are metallic, made of steel. The grout is made of a high performance cementitious (UHPC) material developed specifically for grouted structural connection Ducorit S5. The model allows showing the propagation of the AE wave due to defect initiation or growth. The acoustic emission is modelled as a transient displacement of a crack line in the grout (red line Figure 6).

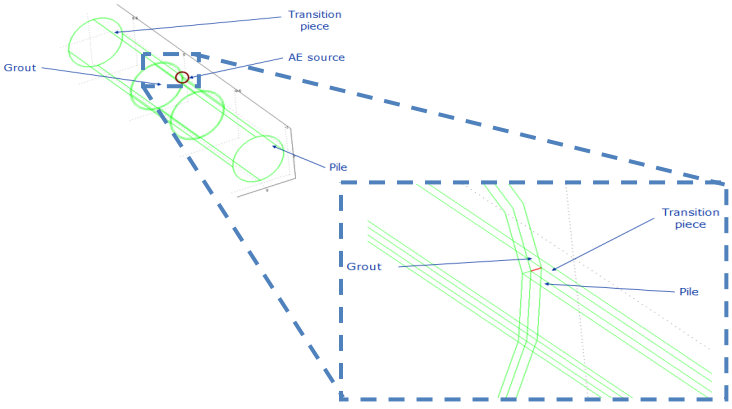

$$u(t) = \begin{cases} \sin 2\pi f t \left(1 - \cos 2\pi \frac{f}{n} t\right) & t \le \frac{n}{f} \\ 0 & t \ge \frac{n}{f} \end{cases}$$

Figure 6: Modelling of the AE source.

The release of elastic energy when a defect such as a crack is opening leads to release of energy and its transformation into kinetic energy. The transient vibrations initiation in the defect is modelled as a transient displacement. The transient displacement is characterized by its frequency (f) and the number of cycles (n) and is given by the following expression:

3.1 Signal attenuation in the grout

The excitation applied was the same frequency range as the one used on the experimental tests (200kHz). The attenuation in the material is simulated using the linear bulk viscosity coefficient. The wave propagation from an AE event is shown in Figure 7.

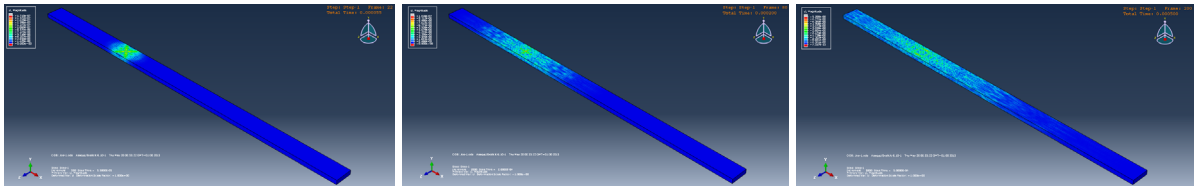

Figure 7: Wave propagation after 0.055ms, 0.2ms and 0.5ms.

In order to model the attenuation in the grout, the structural damping factor has been used, but did not show any correlation between simulations and experiments. Alternatively, a parametric study was performed to correlate the experimental attenuation with simulations using the bulk viscosity parameters as shown in Table 2.

Linear bulk viscosity	Peak excitation (m)	Peak sensor U2 (m)	Attenuation (dB)
0.06	0.000002	3E-10	76.47817482
0.04785	0.000002	7E-10	69.11863911
0.0194	0.000002	5.63E-09	51.01043202
0.0184	0.000002	6.06E-09	50.37114743
0	0.000002	0.00000004	33.97940009

Table 2: Sensitivity of the AE attenuation in the grout at 1m to the linear bulk viscosity.

The attenuation at 1m varies almost linearly with the linear bulk viscosity. The 50dB attenuation was obtained for a linear bulk viscosity of 0,0184MPa.

3.2 Signal attenuation in the steel

The same procedure was used for steel in order to estimate the attenuation. The simulation was carried out on the plate used in the mock-up. In order to limit the size of the computation, half the plate modelled with the symmetry boundary condition used to simulate the other half. The meshing was performed using elements of 5mm.

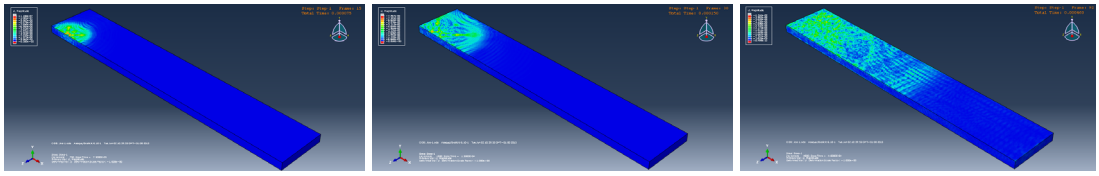

Figure 8 Wave propagation after 0.07ms, 0.15ms and 0.46ms.

Linear bulk viscosity	Peak excitation (m)	Peak sensor (m)	Attenuation (db)
0	2.00E-06	1.50E-08	42
1.00E-12	2.00E-06	1.40E-08	43
0.003	2.00E-06	1.28E-08	44
0.015	2.00E-06	1.00E-08	46

Table 3 Sensitivity of the AE attenuation in the metallic plate to the linear bulk viscosity

Results reveal that with the linear bulk viscosity parameter at 0, the dispersions of the intensity signal is enough to overcome the value of attenuation desired.

4 SIMULATION OF THE ATTENUATION IN THE REAL STRUCTURE

In order to simulate the attenuation over a long distance (7m) and due to the considerable size of the structure, infinite elements and symmetry was used. The model in Figure 9 shows that an AE source is simulated inside the grout. On the later boundaries, an infinite boundary condition is fixed preventing any reflection in the transition piece and the pile laterally. The only reflections and refractions happening occurs at the interface between the pile and the grout on one hand and the grout and the transition piece on the other hand. The near face has a symmetry Boundary Condition applied in the ‘Z’ direction, such that the AE point source

was completely embedded in the centre of the grout layer.

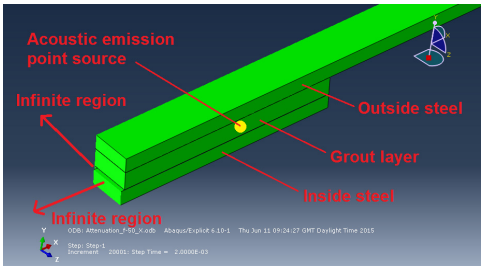

Figure 9: Finite element model geometry and features.

The Acoustic Emission source consisted of a sine excitation of eight cycles and frequencies of 50kHz, and 200kHz. In Abaqus, this amplitude was applied to a fixed point in the grout layer as a mono-polar displacement in a single axis; both 'X' and 'Y' directions were tested. The magnitude of the excitation is one micrometre.

Displacement outputs are generated over a time of two microseconds from single points on the top surface of this layer. These points were positioned in increments of 10cms within the first metre of length, and in increments of 50cms within the remaining nine metres of length, with the starting point '0cm' directly above the position of the AE source.

Figure 12 shows the displacement in the x (U1) and y (U2) at the surface of the pile due to AE emission at different distances from the AE source (20cms to 7m). The important displacement here is U2 as it is normal to the surface and is the main component detected by the AE sensors. The frequency used for AE transmission is 200kHz.

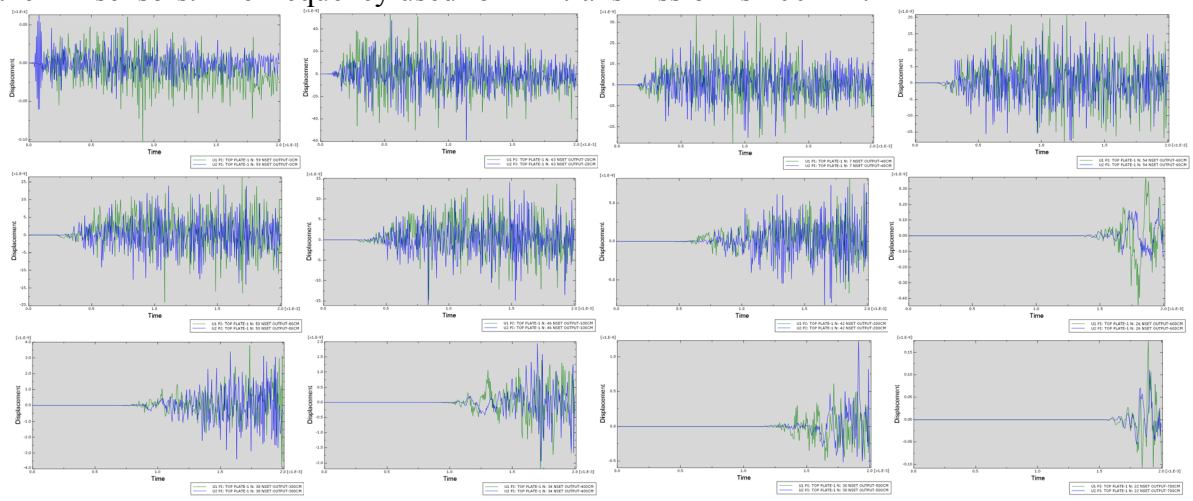

Figure 10: Displacement on top of the source of AE in the pile and displacement at 20cm, 40cm, 60cm, 80cm, 1m, 2m, 3m, 4m, 5m, 6m and 7m from the source of AE in the pile.

Based on the simulations results, the amplitude attenuation of the AE wave due to both geometrical and structural damping depending on the amplitude of the AE source (in dB). Due to the use of infinite elements, there were no reflexions due to the edges of the structure. Indeed the structure is infinite laterally. The only reflections and refractions occur at the interface between the grout and the metallic plates encapsulating it (pile and transition piece).

The parameters governing the coverage of the AE sensors are the noise levels and the energy released by the defects. The attenuation of the AE wave displacement as it propagates in the pile of the tower. These results showed that the direction of opening of cracks (x or y) does not affect the amplitude or the attenuation of the AE wave as it propagates. The 200kHz wave

showed higher attenuation at the beginning which is due to the scattering of the wave, the attenuation at higher distance is not significantly different from the results obtained with the 50kHz AE source.

4.1 Simulation of the test mock-up

The determination of the properties of both the steel and the grout did allow the simulation of the propagation of a defect initiated in the grout and which propagation is picked by AE sensors in the steel. The mock-up was simulated as shown in Figure 11.

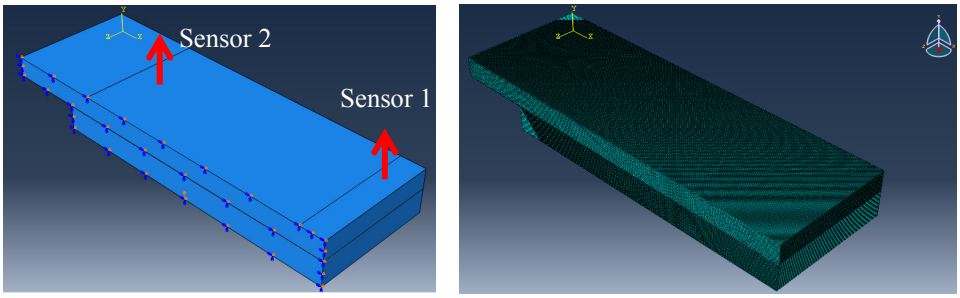

Figure 11a. Modelling of AE in the mock-up. b. Meshing of the mock-up.

In Figure 11a, only half the mock-up is modelled. The symmetry condition is applied in order to simulate half the mock-up only allowing finer meshing and reducing the computation time. The mesh size is very fine with a 2mm element size. The propagation of the AE wave is shown as it moves from the grout to the steel on top at different times in Figure 12.

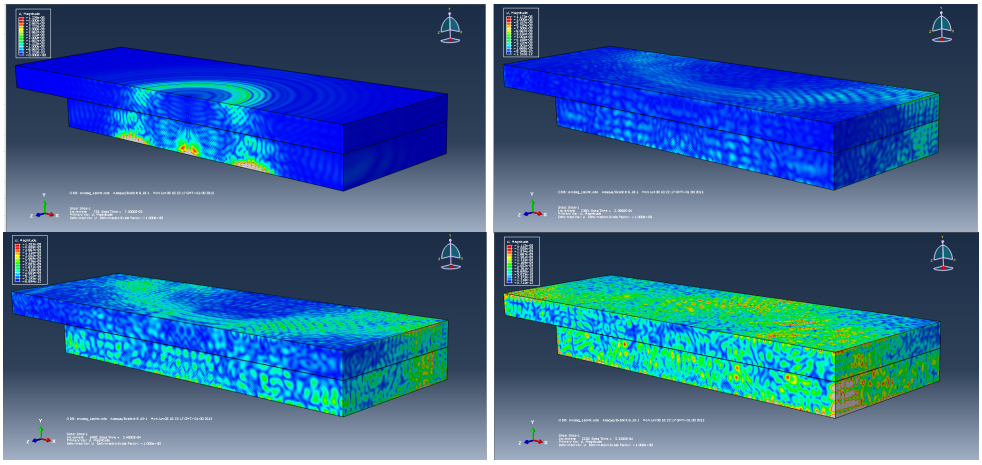

Figure 122 Wave propagation in the mock-up at a. t=7.2 10-5s. b. t=2.39 10-4s.c, t=2.4 10-4. d. t=3.32 10-4.

The AE energy was generated in the grout. It propagated towards the steel plate, some of the energy was dissipated in the grout during the process. The AE wave hit the plate at different angles leading to mode reconversion and different times of propagation depending of the angle at which the wave hits the surface. Speed propagation in the grout was lower than in the steel. The effect of this is that the transmitted AE wave to the steel is dilated over time with smaller peak amplitude. In simulations, comparing the AE signal from the grout and steel and the AE signal in the grout, the effect of the diffraction was well shown with the signal showing a lot of peaks due to diffraction and a lower peak amplitude (higher attenuation). The attenuation (reduction in peak amplitude) is not mainly physical (structural damping in grout), it is due to diffraction leading to the energy being spread over time and resulting in peak amplitude decrease. The attenuation of the AE wave was found to be 55.8dB in Sensor1 and 55.28dB in Sensor 2.

3.5 Conclusion

The correlation between simulation and measurements using Abaqus showed it possible to model Acoustic Emission using the linear bulk viscosity. Based on this parameter and on simulations performed using Abaqus, it was possible to determine the coverage of each sensor depending on the localisation technique, the frequency of the sensor (50kHz or 200kHz), the amplitude of the AE sources we would like to detect and the noise levels.

4 CONCLUSIONS

The challenge of detecting AE emission coming from defects in the grout is the high attenuation of AE waves in cements generally. Measurements were carried out on a test mock-up and speed propagation and attenuation results observed allowed the correlation with the simulations.

The use of the linear bulk viscosity in simulations allowed correlating the attenuation of the AE wave with measurements. Subsequent simulations of the propagation of AE wave in the tower structure allowed the determination of the area of coverage of each AE sensor based on noise levels, AE source minimum signal amplitude and localization technique. Based on the sensor selection and the size of the area monitored as well as the AE location technique used (zonal or geometric), this will ultimately determine the number of hardware needed (number of channels for DAQ, number of sensors and their positions).

REFERENCES

[1] "*Acoustic Emission Health Monitoring of Marine Renewables*", J. Walsh, I. Bashir, P. R. Thies, L. Johanning. (2015).

[2] "*Remote Monitoring of Offshore Structures using Acoustic Emission*", D. Duthie, F. Gabriels. 11th European Conference on Non-Destructive Testing (ECNDT 2014)